J. COMBIN. MATH. COMBIN. COMPUT. 127b (2025) 4029--4054

Journal of Combinatorial Mathematics and Combinatorial Computing
www.combinatorialpress.com/jcmcc

Combinatorial Press

Research on intelligent operation and maintenance of electrochemical energy storage plant based on multimodal fusion sensing technology

Chao Dong[1,✉], Bangjin Liu[1], Min Zhang[1], Linwei Wang[1], Liangrui Zhou[1], Bo Zhao[1]

[1] *CGS POWER GENERATION (GUANGDONG) ENERGY STORAGE TECHNOLOGY CO., LTD., Guangzhou, Guangdong, 510630, China*

ABSTRACT

In order to realize the intelligent operation and maintenance of electrochemical energy storage power station and make the working process of the power station battery more efficient, stable and safe, this paper establishes a safety monitoring system of electrochemical energy storage power station through multimodal fusion sensing technology. The multi-sensor fusion technology and multi-sensor calibration process are proposed, and the Kalman joint filter fusion algorithm is obtained based on the traditional Kalman filter extension, which fuses the collected multi-modal sensing data to realize the real-time detection of the state information of each battery of the energy storage power station. Simulation experiments are carried out to verify the reliability of the Kalman joint filter fusion algorithm, and the deviation value of this algorithm in the filter fusion processing is only 0.1426, which is lower than that of the comparative sliding average filtering algorithm. The RMSE values of X-axis and Y-axis in the motion target tracking experiments are less than those of the comparative mean drift algorithm 0.189 and 0.1412, and in the speed, they are less than those of 0.0062 and 0.0073, which are better in terms of accuracy performance. And in the application practice of battery safety monitoring system for electrochemical energy storage power station, the error between SOC estimation and actual value is less than 5% in either DST condition or UDDS condition, and the internal resistance R_0 change curve is similar to the actual value of the internal resistance, and the estimation error is less than 4%.

Keywords: Multimodal fusion sensing technology, multisensory, Kalman filter, battery safety monitoring

1. Introduction

With the transformation of the global energy structure and the large-scale development and utilization

✉ Corresponding author.
E-mail address: cnkjdongchao@126.com (C. Dong).

Received 20 February 2024; Revised 05 April 2024; Accepted 20 November 2024; Published Online 16 April 2025.
DOI: 10.61091/jcmcc127b-223

of renewable energy, the problems of volatility, intermittency and uncertainty of the power grid are becoming more and more prominent [1-2]. In this context, electrochemical energy storage power plants play an increasingly important role in stabilizing power grids, shaving peaks and filling valleys, and regulating frequency and phase due to their characteristics of fast response, high efficiency energy storage, and environmental protection and non-pollution [3-4]. Especially in the construction and operation of large-scale energy storage power plants of 100 MW level, how to develop scientific and effective scheduling and control strategies has become a hotspot and a difficult point of research in the current energy field [5-6].

However, the development of scheduling and control strategies for large-scale electrochemical energy storage power plants is not an easy task. On the one hand, the electrochemical energy storage plant involves the integration and application of the knowledge of electrochemical principles, battery management system, power electronics technology, automatic control system and other fields, which is technically difficult, and on the other hand, the operation of the energy storage plant involves the aspects of grid scheduling, market analysis, operation management, etc., which makes the real-time, accuracy, and economy of the strategy more demanding [7-10]. Foreign countries started earlier in the technological research and development and application of electrochemical energy storage power plants, and have accumulated certain experience. Developed countries have achieved remarkable results in the scheduling and control strategies of energy storage power plants, realizing the transformation from theoretical research to practical application [11-13]. In contrast, China's research and application in this field is still in its infancy, and although the national and local governments have introduced a series of supportive policies in recent years to promote the construction and development of energy storage power plants, the research on scheduling and control strategies still faces many challenges [14-16].

With the continuous increase of the installed capacity of electrochemical energy storage power stations, its safety risk and prevention and control issues are getting more and more attention. Electrochemical energy storage can effectively reduce the impact of new energy generation on the power grid by dissipating the impact of high wind and solar power generation through fast charging and discharging when new energy generation is low [17-18]. The periodic maintenance strategy commonly used in energy storage power stations is difficult to detect potential safety hazards in time due to the relatively fixed maintenance cycle, while the number of energy storage components, fault types, and the prevention and control methods of offline detection are time-consuming, costly, and have a large amount of workload in operation and inspection, and low maintenance efficiency, which also brings new safety risks in the process of promoting utilization [19-21]. Therefore, it is necessary to reduce the safety risks of electrochemical energy storage power plants from the source to ensure the scientific and reasonable operation of electrochemical energy storage power plants [22].

As the application scale of electrochemical energy storage systems/stations in electric power systems continues to expand, the issues of safety, reliability, and economy are of great concern to the industry [23]. Exploring and proposing the theoretical methods of digitalization and intelligence in the application process of energy storage and its application technology will effectively improve the safe, stable and economic operation level of energy storage, which is an important practical need [24-25]. However, there is a lack of more systematic analysis and discussion on the improvement of the digital and intelligent level of electrochemical energy storage [26].

From a macro point of view, electrochemical energy storage plant is a very important link in the stabilization of the power grid, so it is very important to understand the positioning of electrochemical storage plant in the power grid and how to promote the further adaptation of the storage plant to the smart grid. Literature [27] discusses the improvement of the cost and benefit of electrochemical energy storage technology, which promotes the wide deployment of energy storage systems, which also provides effective support for the stability of the power grid, and introduces in detail the process of the development of the grid storage station and the energy management system (EMS) architecture, which provides a reference for further in-depth study of the EMS. Literature [28] affirms the contribution of power storage systems to grid stability and efficiency improvement, and is well suited to the operation and maintenance management model of the smart grid, and proposes strategies to promote the further development of power storage systems, such as the implementation of research, development, and demonstration (RD&D) policies to increase the experience of power storage system operation and maintenance and thus reduce the cost of power storage system operation and maintenance, and the investment of investment tax credits to expand the investment in the research and development of power storage systems on the ground.

How to operate electrochemical storage plants stably, safely and efficiently has always been the focus of research in this field, so the research around the battery module of the storage plant (technology, safety management), energy optimization and management (intelligent), energy storage technology is very popular. Literature [29] analyzed the performance of Ant-Lion Optimization Algorithm (ALO), Gray-Wolf Optimization Algorithm (GWO), Krill Swarm Algorithm (KH), and JAYA algorithm for electrochemical power storage (lead-acid (LA), lithium-ion (Li-ion), and nickel-cadmium (Ni-Cd) three types of electrochemical battery technologies) and energy management optimization based on the techno-economic optimization criterion and confirmed the performance of The superiority of JAYA algorithm and pointed out that power cost reduction can significantly reduce the unit power cost. Literature [30] systematically reviews several battery systems for electrochemical energy storage power plants and focuses on the characteristics, materials, electrochemical performance, and cost of these battery systems and emphasizes that the capacity and performance of electrochemical storage power plants are determined by the battery system as well as the system of power conditions. Literature [31] describes the importance of thermal management aspects in electrochemical power storage, and the appropriate operating temperature helps electrochemical power storage devices to perform optimally; therefore, an in-depth analysis of the research literature on thermal management of electrochemical energy devices (including fuel cells, electrolysis tanks, and supercapacitors) is conducted to summarize the physicochemical mechanisms of heat generation in these electrochemical devices, which provides important references for the optimization and management of electrochemical energy storage design. It provides an important reference for the optimization and management of electrochemical energy storage design. Literature [32] discusses the classification and practical application of energy storage technology based on renewable energy power storage system, and explores the factors that affect the operation of the power storage system, the state and the storage capacity, and finally discusses the feasibility of artificial intelligence technology-enabled power storage system configuration and energy control strategy based on the methodology of the literature review, which makes a positive contribution to the construction of digital intelligence for the power storage system. Literature [33] for electrochemical power storage station commonly used lithium-electronic batteries, carried out a battery safety assessment test, based on the results of the study, we learned that the battery storage bin pressure relief plate is unknown, the opening pressure as well as the surrounding obstacles will affect the safety of the battery.

Aiming at the operation and maintenance problems of electrochemical energy storage power stations, this paper proposes multi-sensor fusion technology, an important component of multimodal sensing technology, as the core of the technology, and utilizes Kalman filtering to improve and fuse the multi-sensor data to develop a battery safety monitoring system for electrochemical energy storage power stations. The data fusion function of the multi-sensor fusion technology is discussed in depth, and the segmentation operation, global alignment process and precise alignment process steps are proposed for the calibration problem of multiple sensor combinations. The mathematical model of error covariance matrix and overall optimal estimate of the safety monitoring system of electrochemical energy storage power station is obtained by Kalman joint filter fusion algorithm, and the fusion of multi-sensor data in the health monitoring of energy storage battery is realized. The battery safety monitoring system of electrochemical energy storage station is constructed by combining the ampere-time integration method with the open-circuit voltage method to estimate the charge state of the battery, and the functions of user login screen and main monitoring screen are set up according to the requirements. The reliability of the multi-sensor Kalman joint filter fusion algorithm proposed in this paper is verified by using filter fusion processing and motion target tracking simulation experiments, and the application of this paper's electrochemical energy storage plant battery safety monitoring system is practiced under DST and UDDS conditions.

2. Application of multimodal sensing technology in substation equipment monitoring

In the health condition monitoring of substation equipment, multimodal sensing technology can fuse multiple sensor data such as vibration, temperature, sound and image to provide richer equipment status information [34].

With the continuous expansion of the power grid scale and the continuous improvement of the level of intelligence, the health condition monitoring of substation equipment is particularly important. Traditional monitoring methods often rely on data from a single sensor, which can reflect the state of the equipment to a certain extent, but it is difficult to comprehensively and accurately capture all the state information of the equipment. In order to have a more comprehensive understanding of the operating status of substation equipment and to detect and deal with potential faults in a timely manner, multimodal sensing technology has emerged.

2.1. Vibration monitoring

Vibration monitoring is one of the important applications of multimodal sensing technology in substation equipment monitoring. Through vibration sensors, the vibration signals of the substation equipment can be monitored in real time, and then analyze the operating status and potential faults of the equipment. The vibration signal contains a wealth of information about the operating status of the equipment, such as the rotational speed of the equipment, the load condition, the degree of wear and tear of the components and so on. Through the processing and analysis of vibration signals, the abnormal state of the equipment can be effectively identified, and timely maintenance measures can be taken to avoid the occurrence of failures.

2.2. Temperature Detection

Temperature monitoring is another important application of multimodal sensing technology in substation equipment monitoring. Using infrared temperature measurement technology, the temperature distribution of the equipment can be monitored in real time, and overheating parts can be found, so as to effectively prevent equipment failure.

Infrared temperature measurement technology through the measurement of infrared radiation energy emitted from the surface of the equipment, which will be converted into a temperature value, to achieve non-contact temperature measurement. The technology has the advantages of fast response speed, wide measurement range, high accuracy, etc., and is suitable for real-time monitoring of substation equipment.

Temperature monitoring can not only find the existing overheating problems, but also predict the future temperature trend of the equipment by analyzing the long-term monitoring data. Combined with the monitoring data of other modes, such as vibration, sound, etc., it can evaluate the health status of the equipment more comprehensively, so as to formulate more effective preventive measures. Temperature monitoring can realize remote and real-time monitoring of equipment, reduce the frequency and difficulty of manual inspection, avoid further expansion of failures, and improve maintenance efficiency.

2.3. Sound monitoring

Sound monitoring plays an important role in substation equipment monitoring. Through sound sensors, sound signals can be captured in real time when the equipment is running, and then the characteristics of these sounds can be analyzed to determine whether there is any abnormality in the equipment. Sound monitoring mainly relies on sound sensors, which can capture the sound signals of equipment operation with high sensitivity. These sound signals contain important information about the operating status of the equipment, such as friction, collision and discharge of components. Through the processing and analysis of these sound signals, the abnormal state of the equipment can be effectively identified for timely maintenance measures to provide the basis.

Sound frequency is an important parameter reflecting the vibration state of equipment components. By monitoring the sound frequency, it can determine whether the equipment components are loose, wear and other abnormal states. Sound pattern is also one of the important contents of sound monitoring. Sound pattern monitoring is important for the development of scientific maintenance programs and replacement strategies. Through long-term monitoring and analysis of the sound change trend, the wear trend and prediction of the remaining life of the equipment can be understood, providing a scientific basis for the maintenance and replacement of the equipment.

2.4. Image monitoring

Image monitoring is another important application of multimodal perception technology in substation equipment monitoring. Through the use of high-definition cameras or drone inspection technology, the image information of the substation equipment can be obtained in real time, and then identify the defects and abnormalities in the appearance of the equipment. This monitoring method is characterized by intuition and accuracy, and can provide strong support for equipment maintenance and overhaul.

3. Intelligent operation and maintenance of electrochemical energy storage plant based on multi-sensor fusion

Multi-sensor fusion is an important part of multimodal fusion sensing technology [35]. In practical applications, multimodal sensing technology often needs to rely on multisensor fusion technology to achieve more efficient data processing and decision support.

With the changes in global energy development, more renewable energy sources are entering the power sector, which brings more challenges to the grid connection in the power sector. One of the effective ways to cope with this challenge is to adopt energy storage technology, in which electrochemical energy storage has been rapidly developed with its unique advantages of high efficiency and environmental adaptability. In order to make the working process of electrochemical energy storage plant more efficient, stable and safe, this chapter will take the multi-sensor fusion technology as the basis, combined with Kalman filtering algorithm, to build up the battery safety monitoring system of electrochemical energy storage plant, and realize the intelligent operation and maintenance of electrochemical energy storage plant.

3.1. Multi-sensor fusion technology

Multi-sensor data fusion problem is the basic research content to carry out this research, so it is necessary to understand the basic principles of data fusion and the data fusion algorithms that are currently used more [36]. Data fusion is a technique for comprehensively analyzing and processing data from multiple sensor sources. This section firstly briefly introduces the basic principles and advantages of multi-sensor data fusion, and secondly elaborates on the fusion center structure, data abstraction level and data fusion functions respectively, so as to have a comprehensive understanding of multi-sensor fusion.

Data fusion is not a one-time process for heterogeneous information, but rather multiple and layered, specifically, the main task of each level of processing is to refine the information on the basis of the previous level. According to the degree of abstraction of the fusion method in the fusion system, it can be summarized into the following three types, data level fusion, feature level fusion and decision level fusion.

Data level fusion is the bottom level fusion, which is a coarse-grained fusion process on unprocessed information, i.e., the step of extracting feature vectors is done after fusion. Data layer fusion requires that the sensor data used for fusion must be homogeneous, i.e., the data is derived from the same type of sensor. The unique feature of data layer fusion is that it preserves the most details of the data and can harbor details that are not available in other fusion types. Since the loss of data information is almost zero, it gives better fusion results than other methods. However, there are some disadvantages of this method, such as high computational requirements for computers and poor stability of information.

Feature layer fusion is also known as intermediate fusion, this level of fusion of feature value extraction step before the fusion, that is, Mr. into feature vectors, and then the fusion of the groups of information, and finally other processing of the target. The advantage of this level of fusion is to achieve a certain degree of data compression, processing is faster, and is conducive to the system's requirements for real-time processing. According to its different target sources are divided into two kinds of features and state fusion, the specific methods of the former are K th-order nearest neighbor algorithm and neural networks, etc., which belong to the scope of pattern recognition. The latter mainly uses algorithms such as multi-hypothesis method and joint probabilistic data association algorithms, which are more often reflected in the field of target tracking.

Decision layer fusion, also known as advanced fusion, after each sensor has completed all operations on the original sensor information (including preprocessing, feature extraction, target recognition), the final result is obtained by completing local decision layer fusion operations on the key points of each sensor. Decision layer fusion has many benefits, such as fault tolerance, small computation, small dependence on sensors (can be homogeneous sensors or heterogeneous sensors), real-time and so on. The biggest disadvantage is the high loss of information and the performance is mainly dependent on the preprocessing phase.

3.2. Multi-sensor calibration process

Perception systems should be highly robust in different environments, so the design of perception systems is usually confronted with sensors that have several complementary information. Vision sensors provide a lot of appearance information, while LiDAR sensors are characterized by high accuracy in ranging and can provide 360-degree information, and the characteristics of these two perceptual technologies make them suitable to be used as two parts of a perceptual system to provide complementary information. However, the combination of these two sensors implies a tedious calibration process.

To address this problem, a monocular camera-based calibration method is proposed, which uses multiple planar checkerboards as calibration targets. The whole calibration step is divided into three steps, the segmentation operation, the global alignment process and the precise alignment process.

1) Segmentation operation. This step calculates the normal vector of each point $p_r^i \in P_r$ (P_r is the set of LiDAR sensor data points) by performing a principal component analysis on the K nearest neighbors $N_{K,P_r}\left(p_r^i\right)$. $n_r^i \in R^3$ The set corresponding to each region is obtained by performing a chunking operation on the greedily growing regions from the random seed points P_r^j. When a point $p_r^i \in P_r$ is a neighbor of the seed and its normal vector is similar to that of the seed, then this point is added into the set P_r^j:

$$\exists p_r^m \in N_{K,P_r}\left(p_r^i\right): p_r^m \in P_r^j \wedge n_r^{iT} n_r^j > \tau_{sgement} \tag{1}$$

Each region is expanded as described above until convergence, then removed from P_r. New seeds are then selected and the above steps are repeated until there are no remaining points in P_r. The final step is to remove segments that are significantly smaller than the checkerboard.

2) Global Alignment. An initial set of transformations $T=\{\theta_j\}$ is generated based on the point cloud data $\{P_c\}$ and $\{P_r\}$ from the vision and LIDAR sensors, respectively.Next, we iteratively randomly select and associate three surfaces from the two sets, compute the transformations, and validate them using a distance metric.

3) Precise Alignment. In the previous step the initial transformation set T was obtained based on the center of mass and normal vector of the point clouds $\{P_c\}$ and $\{P_r\}$. This is fast but not accurate enough, so in this step all transformations $\theta \in T$ make the following error function refined by gradient descent:

$$E(\theta)=\sum_{p_c^c \in P_c}\left\|\tilde{p}_c^i-N_{1,p_t}\left(\tilde{p}_c^i\right)\right\|^2, \tilde{p}_c^i=R\cdot p_c^i+t \tag{2}$$

This minimizes the sum of the point-to-point distances to the nearest neighbors, which can be solved using the well-known iterative nearest-point algorithm. The final result is a set of finely aligned transformations Γ.

The method ends up with six rigid transformation parameters $\theta=\left(r_x,r_y,r_z,t_x,t_y,t_z\right)^T$ to represent the coordinate system of the visual sensor relative to the LiDAR. The method can be used to transform the coordinates p_c of the data points of the visual sensors to the coordinates in the LiDAR by using equation (3) p_r. Where, is the corresponding rotation matrix and is the translation vector.

$$p_r = R_\theta \cdot p_c + t_\theta \tag{3}$$

This calibration method uses a randomized approach in the selection of seeds, which leads to a strong randomness in the accuracy of the calibration results. Moreover, this calibration method requires adjusting the angle of the board according to the parameters of the sensor, and the accuracy of the results strongly depends on the parameters of the sensor or the structural nature of the environment, and thus lacks a certain degree of generalization ability.

3.3. Fusion method for multi-sensor Kalman filtering

3.3.1. Principles of Traditional Kalman Filtering Algorithm.Kalman filtering algorithm is an algorithm that obtains observation information through sensors, makes optimal estimation of the target, and obtains the state or real signal of the target system [37]. The state equation and the measurement equation are the important components of the Kalman filtering algorithm. Most of the information acquired by the energy storage battery health monitoring system is time series discrete data, therefore, the target systems are all assumed to be discrete systems.

1) System model.In the traditional Kalman filtering algorithm, the linear differential equation of the general discrete system state is expressed as:

$$X(k)=\Phi(k)X(k-1)+G(k)U(k)+W(k) \tag{4}$$

where $\Phi(k)$ denotes the target transfer matrix parameters at moments $k-1$ to k, $X(k)$, $X(k-1)$ denote the target state at moments k and $k-1$, $G(k)$ denotes the target control matrix parameters at moment k, $U(k)$ denotes the known input signal, $W(k)$ denotes the process Gaussian white noise which satisfies a Gaussian distribution, and $Q(k)$ is the noise covariance. There are:

$$E[W(k)]=0 \tag{5}$$

$$E\left[W(k)W(k)^T\right]=Q(k)\delta_{kj} \tag{6}$$

where δ_{kj} denotes the Kronecker delta function.

The measurement equation of the system is expressed as:

$$Z(k) = H(k)X(k) + V(k) \tag{7}$$

where $Z(k)$ denotes the measured value obtained by the sensor at moment k, $H(k)$ denotes the measured system parameters, $H(k)$ is the matrix when the measured system is a multi-sensor system, and $V(k)$ denotes the measured Gaussian white noise, which also satisfies the Gaussian distribution, and similarly has:

$$E(V(k)) = 0 \tag{8}$$

$$E\left[V(k)V(k)^T\right] = R(k)\delta_{kj} \tag{9}$$

$$E\left[W(k)V(k)^T\right] = 0 \tag{10}$$

From the above equation, it can be seen that any moment process noise, any moment measurement noise are independent of each other.

2) Algorithm flow.The next state prediction equation of the state is:

$$\hat{X}(k|k-1) = \Phi(k)X(k-1|k-1) + G(k)U(k) \tag{11}$$

In turn, the next prediction equation for the quantitative measurements is obtained as:

$$\hat{Z}(k|k-1) = H(k)\hat{X}(k) \tag{12}$$

The difference between the true value of the measure and the predicted value of the measure is found to be:

$$\gamma(k|k-1) = Z(k) - Z(k|k-1) \tag{13}$$

The error covariance equation for one-step state prediction is:

$$P(k|k-1) = \Phi(k)P(k-1|k-1)\Phi(k)^T + Q(k) \tag{14}$$

The state prediction covariance equation $P(k|k-1)$ represents the uncertainty of the state prediction, with smaller values indicating higher accuracy of the predicted state data.

The covariance equation of one-step measurement prediction is:

$$S(k) = H(k)P(k|k-1)H(k)^T + R(k) \tag{15}$$

The measurement prediction covariance equation $S(k)$ indicates the uncertainty of the measurement prediction, and the smaller its value, the higher the accuracy of the predicted measurement data.

From equations (14) and (15), the filtering gain matrix is obtained as:

$$M(k) = P(k|k-1)H(k)^T S(k)^{-1} \tag{16}$$

This in turn leads to the state update equation at moment k:

$$X(k|k) = \hat{X}(k|k-1) + M(k)\gamma(k|k-1) \tag{17}$$

In order for the Kalman filter to keep updating, it is also necessary to find the covariance equation for updating the next step:

$$P(k|k) = [I - M(k)H(k)]P(k|k-1) \tag{18}$$

where I denotes a unit matrix with the same covariance dimension.

3.3.2. Principles of Kalman Joint Filter Fusion Algorithm. On the basis of traditional Kalman filtering, the Kalman joint filter fusion algorithm is obtained by extension. Multi-sensor data fusion technology utilizes Kalman joint filter fusion algorithm to fuse the collected data of multi-sensors, and its main algorithm derivation process is as follows.

1) System Model. When the system consists of N sensor, the sensors are independent of each other, and the state linear differential dynamic equation of each sensor is expressed as:

$$X_i(k) = \Phi(k \mid k-1) X_i(k-1) + G(k)U(k) + W(k) \tag{19}$$

Eq. (19) is the state equation of the i nd sensor, where $X_i(k)$ denotes the system state at the k th moment of the i th sensor, $\Phi(k \mid k-1)$ denotes the transfer matrix from the $k-1$th moment to the k th moment, $G(k)$ denotes the parameters of the target control matrix, $U(k)$ denotes the control matrix, and $W(k)$ denotes the process Gaussian white noise sequence, whose mathematical-statistical distribution is:

$$W(k) \sim N[0, Q(k)] \tag{20}$$

When the monitoring system is arranged with N sensor, the measurement equation of the sensor is:

$$Z_i(k) = H_i(k) X_i(k) + V_i(k) \tag{21}$$

where $i = 1, 2, \cdots, N$, $Z_i(k)$ denote the observations collected by the i rd sensor, $H_i(k)$ denotes the measured system parameters of the i th sensor, and $V_i(k)$ denotes the measured Gaussian white noise sequence of the i th sensor with the mathematical statistical distribution:

$$V_i(k) \sim N\left[0, R_i(k)\right] \tag{22}$$

It is easy to see that the process noise at any moment and the measurement noise at any moment are independent of each other.

The initial value of the target state is $X(0)$, and its mean value is X_0, which can be known:

$$E[X(0)] = X_0 \tag{23}$$

$$E\left[\left(X(0) - X_0\right)\right]\left[\left(X(0) - X_0\right)^T\right] = P_0 \tag{24}$$

It is assumed that the measurement of Gaussian noise $V_1(k), V_2(k), \cdots, V_N(k)$, process noise $W(k)$ and $X(0)$ are equally independent from each other.

In summary, in order to represent the total measurement equations for all sensors uniformly, Eq. (21) can be written as:

$$Z(k) = H(k) X(k) + V(k) \tag{25}$$

Its mathematical and statistical distribution has:

$$V(k) \sim N[0, R(k)] \tag{26}$$

Among them:

$$\begin{aligned} Z(k) &= \left[Z_1^T(k), Z_2^T(k), \cdots Z_N^T(k)\right]^T \\ H(k) &= \left[H_1^T(k), H_2^T(k), \cdots H_N^T(k)\right]^T \\ V(k) &= \left[V_1^T(k), V_2^T(k), \cdots V_N^T(k)\right]^T \\ R(k) &= diag\left[R_1(k), R_2(k), \cdots R_N(k)\right] \end{aligned} \tag{27}$$

2) Algorithm flow. After the overall optimal estimate $X(k-1 \mid k-1)$ and error covariance $P(k-1 \mid k-1)$ of the state at the moment $k-1$ of the previous step are known, when the measured

values of all the sensors at the moment k are obtained, the error covariance matrix (28) and the overall optimal estimate (29) and of the system are obtained by the basic algorithm of Kalman filtering and there are [38]:

$$P^{-1}(k|k) = P^{-1}(k|k-1) + \sum_{i=1}^{N} \left[P_i^{-1}(k) - P_i^{-1}(k|k-1) \right] \tag{28}$$

$$\begin{aligned} X(k|k) &= P(k|k)P^{-1}(k|k-1)\hat{X}(k|k-1) \\ &+ P(k|k)\sum_{i=1}^{N} \left[P_i^{-1}(k|k)X_i(k|k) - P_i^{-1}(k|k-1)\hat{X}_i(k|k-1) \right] \end{aligned} \tag{29}$$

Among them:

$$X_i(k|k) = \hat{X}(k|k-1) + M_i(k)\gamma_i(k|k-1) \tag{30}$$

$$\hat{X}(k|k-1) = \Phi(k|k-1)X(k-1|k-1) + G(k)U(k) \tag{31}$$

$$P_i(k|k-1) = \Phi(k|k-1)P_i(k|k)\Phi(k|k-1)^T + Q(k-1) \tag{32}$$

$$M_i(k) = P_i(k|k-1)H_i(k)^T \left[H_i(k)P_i(k|k-1)H_i(k)^T + R_i(k) \right]^T \tag{33}$$

$$\gamma_i(k|k-1) = Z_i(k) - \hat{Z}_i(k|k-1) \tag{34}$$

$$P_i(k|k) = \left[I - M_i(k)H_i(k) \right] P_i(k|k-1) \tag{35}$$

The above equations (30) to (35) can be calculated by the conventional Kalman filtering algorithm.

In the above Kalman joint filter fusion algorithm for multi-sensor data fusion, when the overall optimal estimate $X(k-1|k-1)$ and error covariance $P(k-1|k-1)$ of the state at the moment $k-1$ of the previous step are known, and the measured values of all the sensors at the moment k are obtained, the formulas of error covariance matrix and overall optimal estimate of the system are obtained by the Kalman joint filter fusion algorithm, and the multi-sensor data of the energy storage battery health monitoring is realized. Fusion.

Kalman joint filter fusion algorithm is assumed in various engineering industry applications:

$$P^{-1}(k|k-1) = \sum_{i=1}^{N} P_i^{-1}(k|k-1) \tag{36}$$

Equation (28) can be simplified as:

$$P^{-1}(k|k) = \sum_{i=1}^{N} \left[P_i^{-1}(k|k) \right] \tag{37}$$

There is:

$$P(k|k) = \left\{ \sum_{i=1}^{N} \left[P_i^{-1}(k|k) \right] \right\}^{-1} \tag{38}$$

Therefore, equation (29) simplifies to have:

$$X(k|\ k) = P(k|\ k)\sum_{i=1}^{N} P_i^{-1}(k|\ k)X_i(k|\ k) \tag{39}$$

3.4. Development of safety monitoring systems for electrochemical energy storage plants

The electrochemical energy storage power station safety monitoring system, also known as the intelligent battery manager, plays the role of connecting the energy storage battery and the user.

Through the real-time detection records of the system platform, the user can view and understand the operation of each sub-cell in the battery cluster in real time, extend the service life of the battery, reduce the probability of accidents that may occur in the course of the battery's work, and then ensure that the entire power system works in a healthy and stable manner. With the in-depth development of energy storage technology, safety monitoring system has become an indispensable part of the entire power system. The key point in the development of battery safety monitoring system for energy storage power station is how to monitor the status of each sub-cell in the energy storage battery cluster in real time and manage it accordingly. Large-capacity battery clusters require higher consistency for each battery, and in the real test, the performance of lithium batteries will have a certain gap after many runs, which makes the performance of the whole battery system deteriorate, affecting the battery's use time and the charge state of battery clusters SOC. The safety monitoring system for energy storage plant developed in this paper mainly includes battery temperature acquisition module, battery voltage acquisition module, battery current acquisition module, environmental humidity acquisition module and ZigBee communication module.

Estimation of Battery State of Charge Using the Ampere-Time Integration Method SOC The Ampere-Time Integration Method (ATIM) does not take into account the internal acting mechanism of the battery, and estimates the state of charge of the battery by integrating the time and current, and sometimes adding certain compensation coefficients, according to certain external characteristics of the system such as the current, time, and temperature compensation to compute the total amount of power flowing into/out of the battery. Currently the ampere-time integration method is widely used in battery management systems, and its calculation formula is as follows:

$$SOC = SOC_0 - \frac{1}{C_E}\int_0^t \eta I(t)dt \tag{40}$$

Where SOC_0 is the initial power value of the battery charge state, C_E is the rated capacity of the battery, η is the charging and discharging efficiency coefficient, also known as the Coulomb efficiency coefficient, represents the power dissipation inside the battery during the charging and discharging process, with the charging and discharging multiplication rate and temperature correction coefficients as the main factors, $I(t)$ is the charging and discharging current of the battery at the moment of t, and t is the charging and discharging time.

In order to make the accuracy of current measurement improved, high-performance current sensors are usually used to measure the current, but this increases the cost. For this reason, in this paper, the open-circuit voltage method is applied along with the ampere-time integration method to combine the two. The open-circuit voltage method is used to estimate the initial state of charge of the battery, and the ampere-time integral method is used for real-time estimation, and the relevant correction factor is added to the equation to improve the calculation accuracy.

The program design of the upper computer of this system adopts VB6.0 visualization software, and the main programs include hardware initialization, battery state information acquisition, information transfer settings, over-limit alarm, and historical data storage. In order to facilitate further upgrading of the program in the future and improve the readability and efficiency of the program, the corresponding modules are divided according to the types of functions, and the specific software flow is shown in Fig. 1.

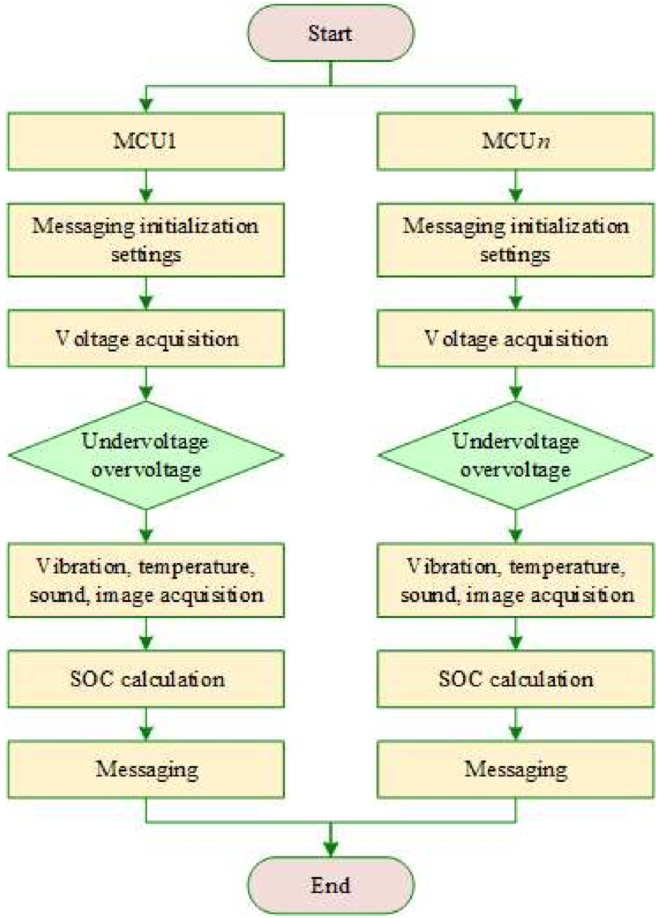

Fig. 1. System software process for battery safety monitoring

According to the functional needs of the system, the monitoring screen of this software includes the user login screen, the main monitoring screen, the battery pack information screen, the alarm information screen, the historical data screen, etc., as follows.

1) User login screen. After opening the control software, the user first clicks the "User Login" button to enter the login screen. Only after correctly entering the user name and password to log in, the user can enter the main monitoring screen of the software, and then utilize the system to realize monitoring, operation or management.

2) Main monitoring screen. The main monitoring screen mainly shows the overall data of the battery of the energy storage power station, and it can also set the relevant parameters and PLC control. The overall data include system status, total voltage, current, maximum voltage, minimum voltage, average voltage, maximum temperature, minimum temperature, maximum humidity, minimum humidity, maximum charge state SOC, minimum charge state SOC.

3) Battery pack information screen. The battery pack information screen is mainly used to display and monitor the voltage, current, temperature, SOC and other information of each battery in real time.

4) Alarm information screen. Alarm information screen is mainly used to display the alarm condition and specific fault information of the monitoring system, and the alarm information is output by default in chronological order in the information summary for the administrator to view in real time.

5) Historical data screen. After opening the historical data screen window, you can query all the data recorded after the activation of the detection system and display the change curve of voltage, current, temperature, humidity, SOC with time for each battery.

4. Multi-sensor filter fusion processing simulation experiment

In the previous chapter, this paper proposes Kalman filtering algorithm to fuse the collected data of multi-sensors to improve the accuracy and fault tolerance of multi-sensor monitoring data. In this chapter, the reliability of the multi-sensor Kalman joint filter fusion algorithm proposed in this paper will be verified through filter fusion processing and motion target tracking simulation experiments.

4.1. Filter fusion processing simulation experiment

Sliding average filtering algorithm is selected as a comparison algorithm, respectively, its and this paper's algorithm on a sinusoidal signal with noise filtering fusion processing, the use of three sensors on the target to measure, to get the waveforms of signals with different fusion methods, as shown in Figure 2. Figures (a) and (b) show the signal waveforms of the sliding average filtering algorithm and this paper's algorithm, respectively.

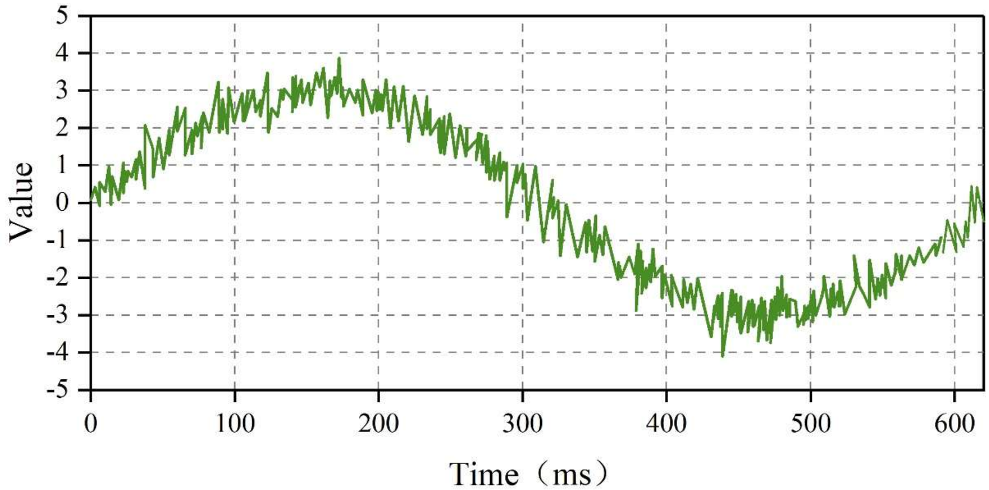

(a)Sliding average filtering algorithm

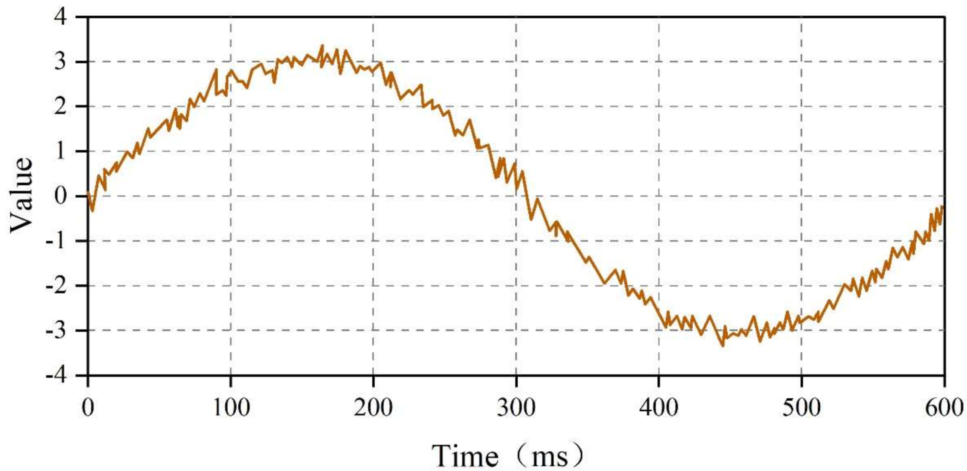

(b)Algorithm of this article

Fig. 2. Signal diagram

The estimation errors obtained by the sliding average filtering algorithm and the algorithm in this paper were analyzed to derive the mean and variance of the error series of the two specifically as shown in Table 1. Where the deviation is quantified as the degree of deviation of the calculated filtered results from the true value. The deviation value of this paper's algorithm is only 0.1426, while the deviation value of the sliding average filtering algorithm is 0.4152, which is significantly higher than this paper's algorithm. It can be clearly seen that the fusion algorithm proposed in this paper is significantly better than the general multi-sensor quantitative fusion method in terms of accuracy, and can obtain relatively accurate estimation results.

Table 1. Mean, variance and deviation

Algorithm	Mean	Variance	Deviation
Sliding average filtering algorithm	0.0065	0.1428	0.4152
Algorithm of this article	0.0043	0.0224	0.1426

4.2. Motion target tracking simulation experiment

In this section, motion target tracking experiments will be carried out to further validate the performance of the multi-sensor Kalman joint filter fusion algorithm proposed in this paper. The comparison algorithm selected for this experiment is the mean-drift algorithm. The target tracking trajectories of the mean-drift algorithm and the algorithm of this paper are obtained through simulation as shown in Fig. 3. From the figure, it can be seen that due to the interference of noise, the mean-drift algorithm can track the target, but the accuracy is not high.

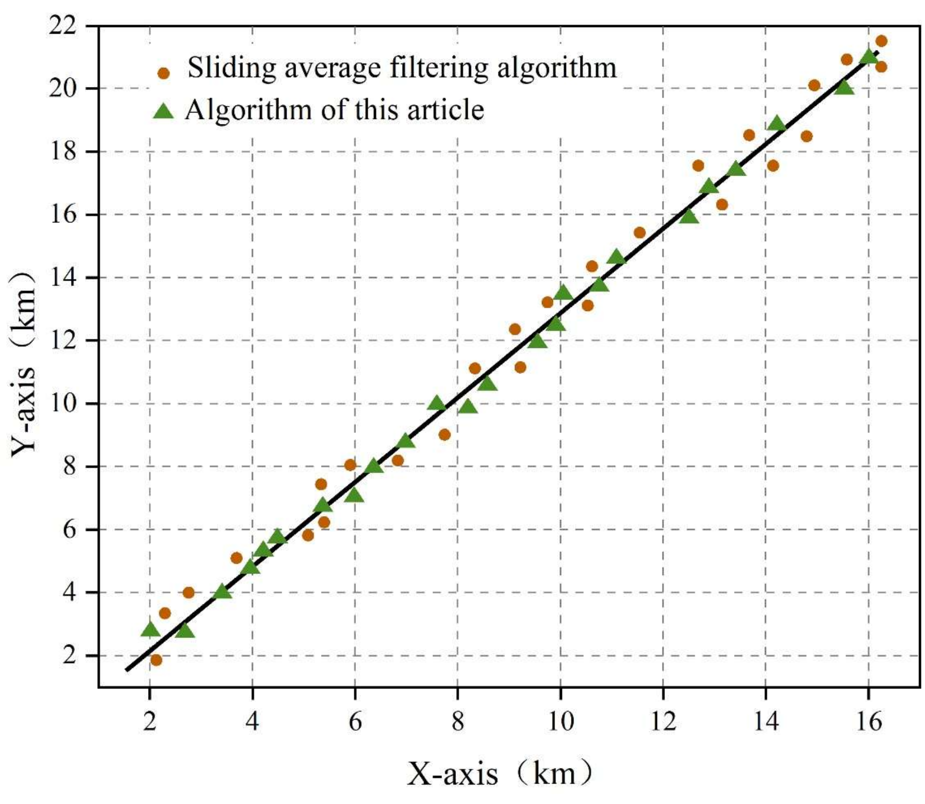

Fig. 3. Target tracking trajectory

Further the root mean square error of the target on the axes and axes when using the mean drift algorithm with the algorithm of this paper for target tracking are given respectively as shown in Fig. 4. Figures (a) and (b) show the root-mean-square error of the position on the X and Y axes, respectively. It can be seen that, with the increase of time, the root mean square error of the position on the axes and axes of the method proposed in this paper is obviously smaller than the general tracking method, which reflects a good anti-interference ability as well as high accuracy.

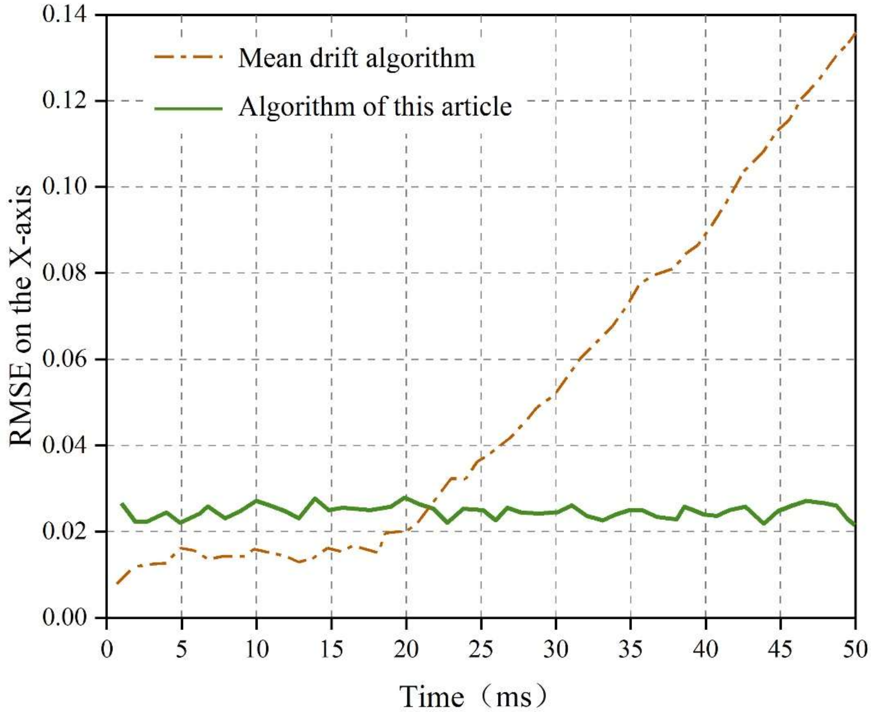

(a)RMSE on the X-axis

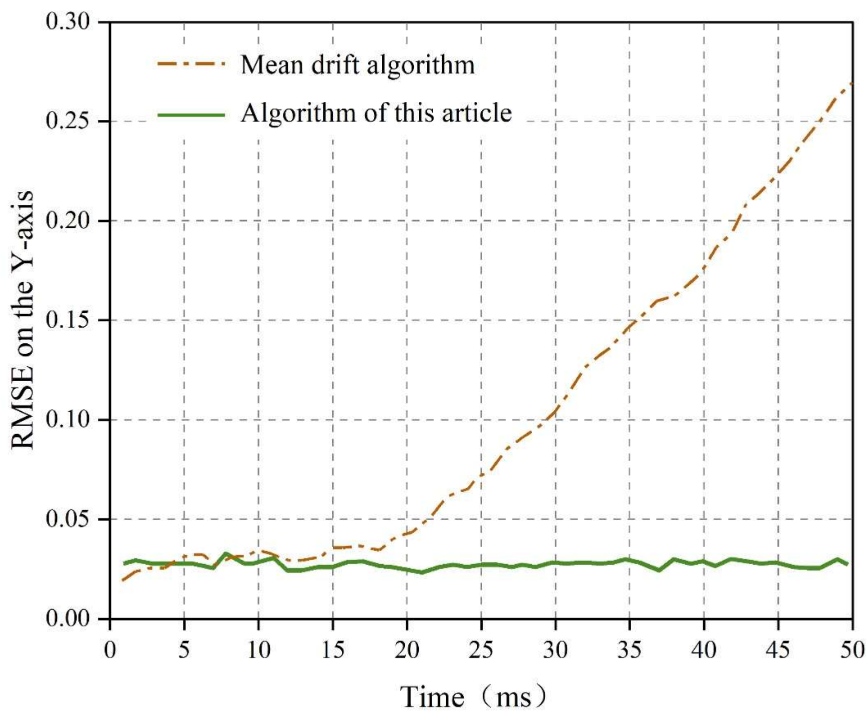

(b)RMSE on the Y-axis

Fig. 4. RMSE on the X-axis and Y-axis

In order to more clearly reflect the superiority of the improved algorithm proposed in this paper in terms of target tracking accuracy, the root mean square error values of the position of the target as well as the root mean square error values (RMSE values) of the velocity are given intuitively, as shown in Table 2. As can be seen from the table, the RMSE values of X-axis and Y-axis of this paper's algorithm are less than those of the mean drift algorithm by 0.189 and 0.1412 for position accuracy, and less than those of the mean drift algorithm by 0.0062 and 0.0073 for velocity, and it is obvious that the proposed improved method is significantly better than the mean drift algorithm in terms of the accuracy of the position and velocity of the tracking of the moving target.

Table 2. RSME

-	-	RMSE	
		Mean drift algorithm	Algorithm of this article
Position(km)	X-axis	0.2538	0.0648
	Y-axis	0.2225	0.0813
Speed(km/s)	X-axis	0.0096	0.0034
	Y-axis	0.0139	0.0066

5. Application of battery safety monitoring systems for electrochemical energy storage power stations

The battery type of electrochemical energy storage power plant is diverse, in which lithium-ion battery becomes the main choice because of its performance advantages, and this chapter of electrochemical energy storage power plant battery safety monitoring object therefore also takes lithium battery as an example. In order to verify the intelligent operation and maintenance performance of the battery safety monitoring system of electrochemical energy storage station constructed in this paper, this chapter will build a simulation model in Matlab/Simulink and apply the system of this paper to accurately detect the battery SOC and internal resistance R_0 of the electrochemical energy storage station in real time, and carry out the experimental validation in the DST condition and UDDS condition, respectively, and characterize the relationship between the definitions of SOH and internal resistance. SOH of Li-ion batteries.The definitions of battery SOC and SOH correspond as follows.
1) SOC. That is, the battery body charging and discharging the battery charge state, the interval is generally controlled to 20%-80%. Generally speaking, lithium battery SOC in the 20% - 80% of the work between the charging and discharging resistance is small, heat is relatively small, resulting in a lower probability of battery overcharge and overdischarge problems.
2) SOH. That is, the state of health of the battery, that is, the service life. General lithium battery SOH decline of 80% must be replaced, too early or too late for battery replacement will have a bad effect, so the battery health state SOH accurate estimation is particularly important. The SOH estimate in this chapter is represented by the characterization parameter of internal resistance R_0 increase.

5.1. Validation of DST working conditions

DST is a dynamic stress test condition obtained by simplifying from the U.S. federal city operating condition FUDS. The equivalent circuit model built in Matlab's simulink is tested by cycling under the DST condition with a step time of 25000S, and the estimated SOC estimate and SOC estimation error value of the estimated lithium battery are shown in Fig. 5, respectively. Figures (a) and (b) are the corresponding SOC estimation and SOC estimation error value plots. SOC1 and SOC2 in Fig. (a) are the actual measured voltage values and the voltage values measured by the detection system in this paper, respectively. From the simulation result graph, it can be seen that in the whole time of simulation, the beginning of the SOC estimation error is larger, is due to the initial value setting is not consistent with the real value, after constantly updating the iteration, the estimated value of SOC is close to the actual value, the error is only about 4%.

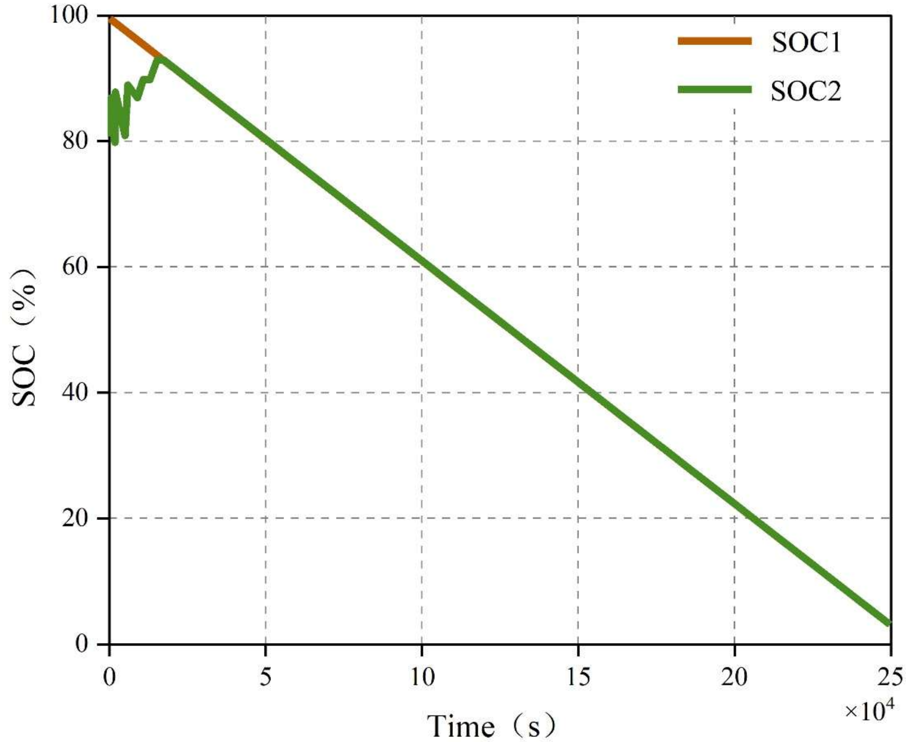

(a)Soc

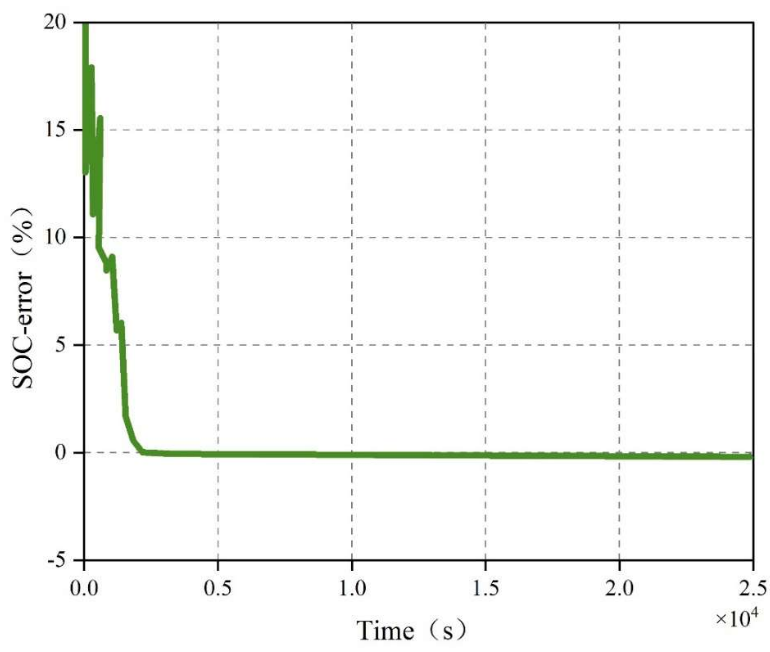

(b)Soc error

Fig. 5. Lithium cell Soc under DST operating conditions

The estimated value of internal resistance and the error value of internal resistance estimation of lithium battery are shown in Fig. 6. Figures (a) and (b) correspond to the internal resistance estimation value and internal resistance estimation error value of the lithium battery. $R_0 1$ and $R_0 2$ in Fig. (a) are the real internal resistance estimation value and the internal resistance estimation value measured by the system in this paper, respectively. It can be seen that, at the beginning of the lithium battery internal resistance R_0 estimation error is larger, but also due to the initial value set in the simulation experiment is not consistent with the real value, after continuous updating iteration, lithium battery internal resistance R_0 estimated value is close to its true value, and can be seen in the figure in a short period of time in lithium battery internal resistance R_0 no significant changes, but with the increase in operating time, lithium battery internal resistance R_0 will slowly grow, lithium battery internal resistance R_0 The change curve is similar to the actual value of internal resistance, and the estimated error is about 3%.

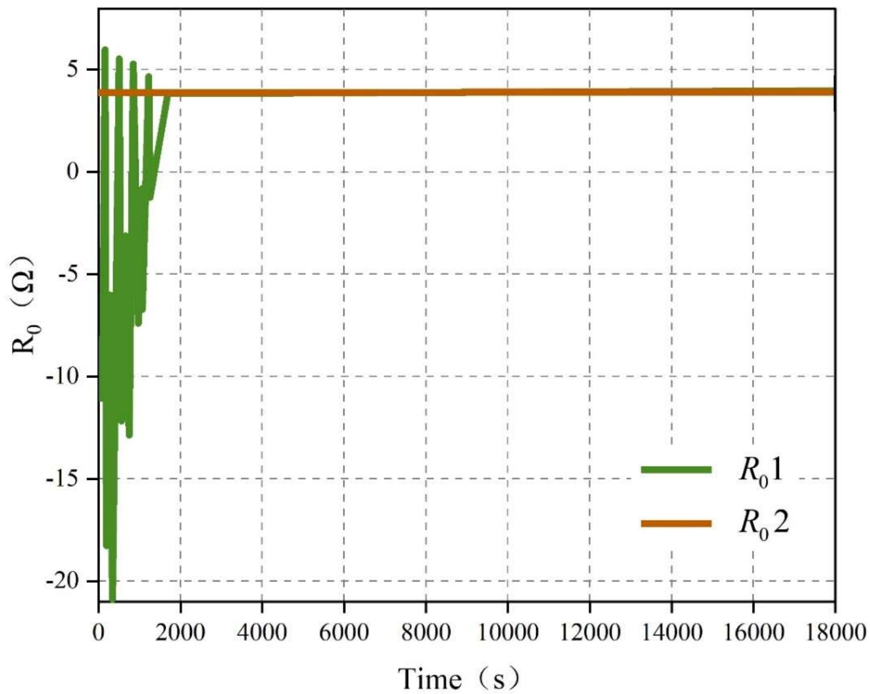

(a) R_0

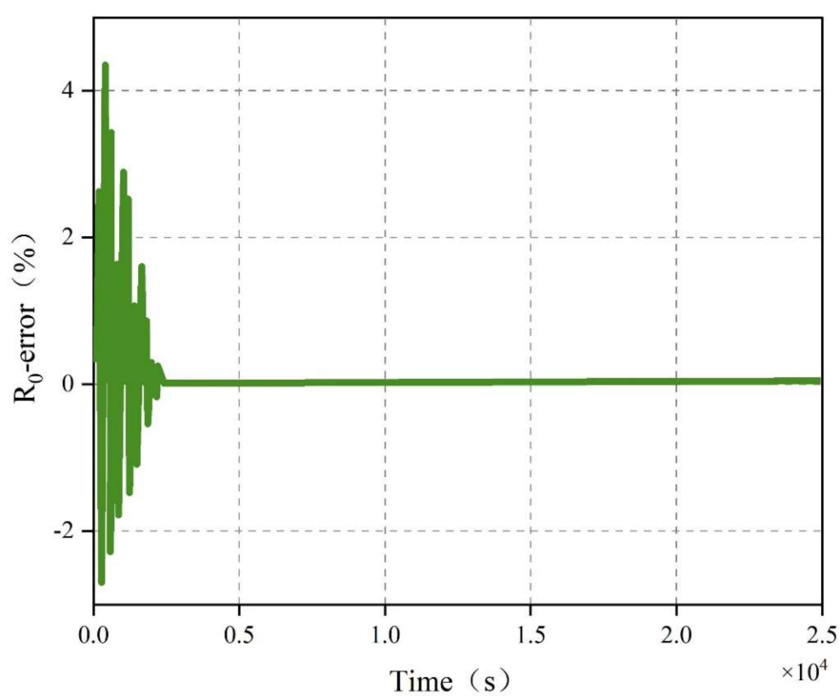

(b) $R_0 - \text{error}$

Fig. 6. Lithium battery internal resistance under DST operating conditions

5.2. Validation of UDDS working conditions

The UDDS condition is an urban road cycle condition developed by the U.S. Environmental Protection Agency (EPA).The estimated SOC and SOC estimation error values of lithium battery under UDDS condition are shown in Fig. 7, respectively. Figures (a) and (b), i.e., the corresponding SOC estimation value and SOC estimation error value are plotted. From the simulation results, it can be seen that in all the time of simulation, the SOC estimation error is larger at the beginning, which is due to the inconsistency between the initial value setting and the real value, and after continuous updating iteration, the SOC estimation value is close to the actual value, and the error is only about 3%.

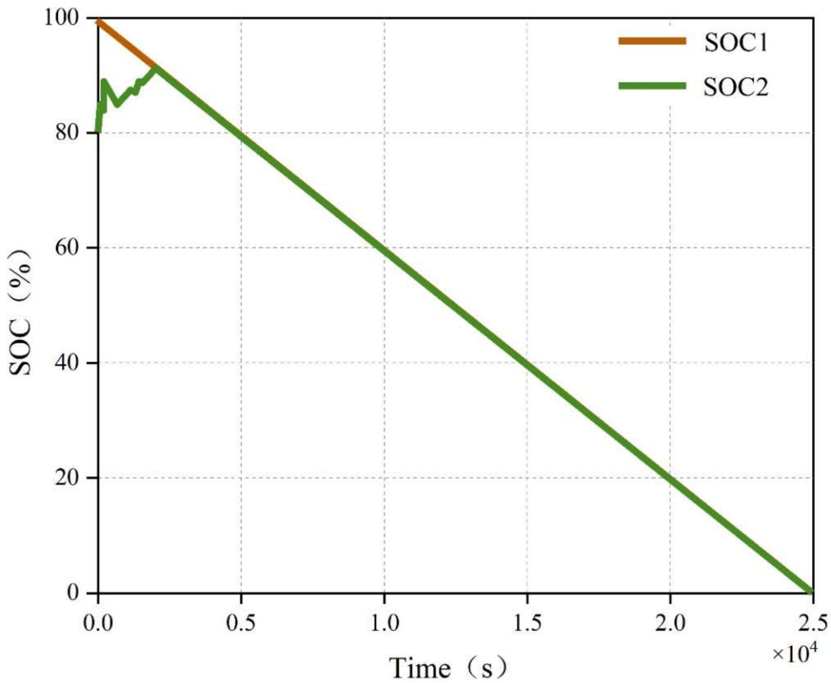

(a)SOC

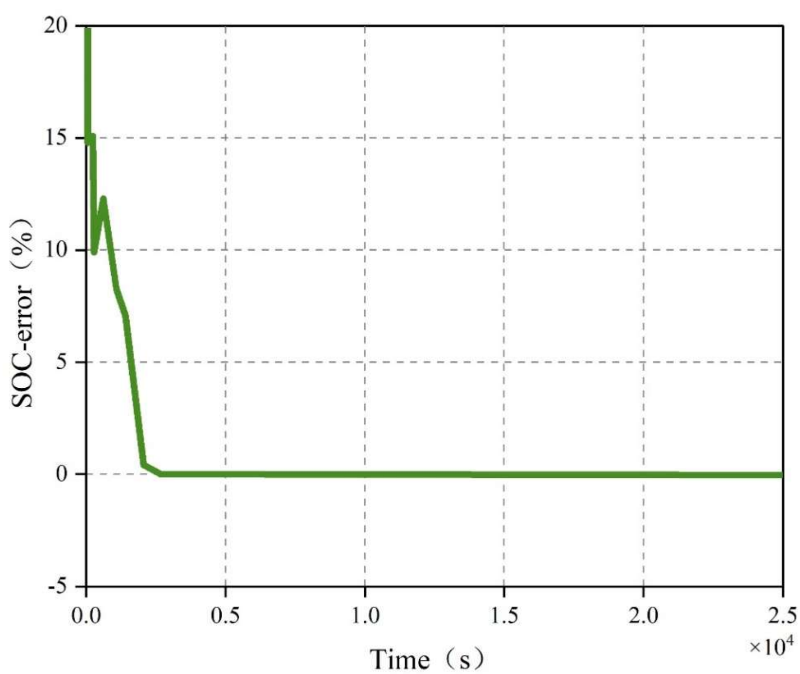

(b)SOC-error

Fig. 7. Lithium cell Soc under UDDST operating conditions

The estimated value of internal resistance and the error value of internal resistance R_0 estimation of the lithium battery are shown in Fig. 8. Figures (a) and (b) correspond to the estimated value of internal resistance and the estimated error value of internal resistance of lithium battery. At the beginning of the lithium battery internal resistance R_0 estimation error is larger, but also due to the initial value set in the simulation experiment is not consistent with the real value, after continuous updating iteration, the lithium battery internal resistance R_0 estimate is close to its real value, and from the figure can be seen in a short period of time lithium battery internal resistance R_0 no significant changes, but with the increase in working time, lithium battery internal resistance R_0 will grow slowly, lithium battery internal resistance 6 change curve and the actual value of internal resistance is similar to the estimated value. The curve of internal resistance R_0 is similar to the actual value of internal resistance, and the estimated error is about 3%.

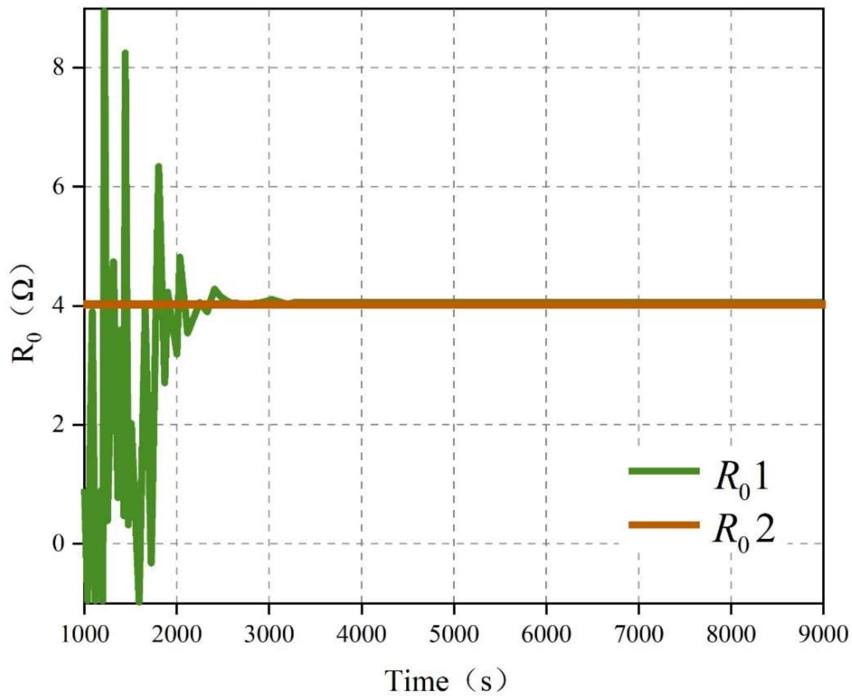

(a) R_0

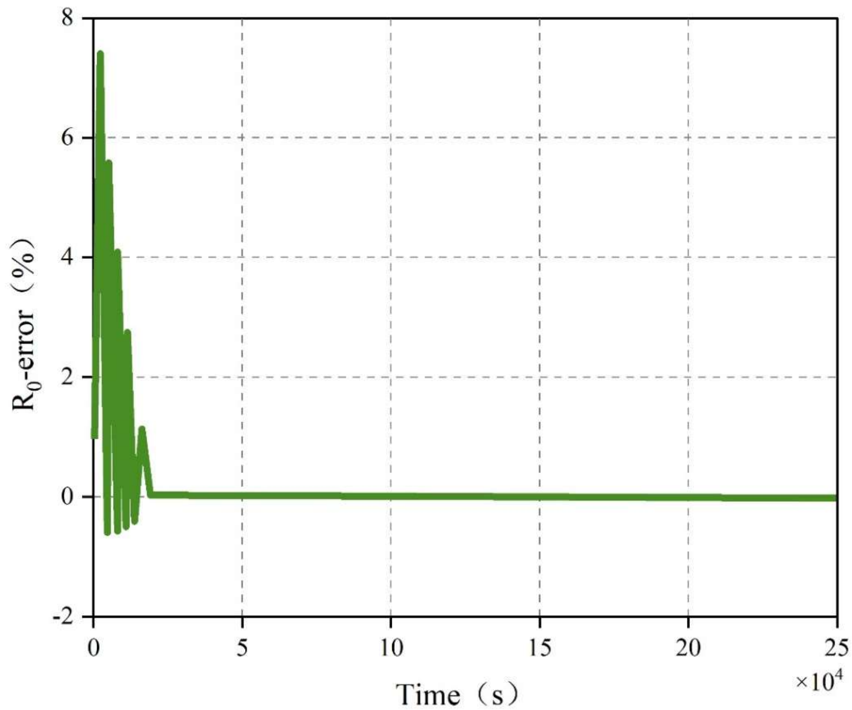

(b) R_0 – error

Fig. 8. Lithium battery internal resistance under UDDST operating conditions

6. Conclusion

Multi-sensor data fusion technology utilizes Kalman joint filter fusion algorithm for multi-modal fusion sensing of multi-sensor collected data to construct a safety monitoring system of electrochemical energy storage power station and realize the intelligent maintenance goal of electrochemical energy storage power station.

In order to verify the reliability of the Kalman joint filter fusion algorithm proposed in this paper, a multi-sensor filter fusion processing simulation experiment is carried out. In the filter fusion processing experiment, the deviation value of the filtering result of this paper's algorithm is 0.142, which is smaller than 0.2726 of the sliding average filtering algorithm, and it performs better in terms of accuracy. This paper's algorithm also still performs well in the motion target tracking experiments, the RMSE values of X-axis and Y-axis are 0.189 and 0.1412 less than the mean drift algorithm, and the speeds are 0.0062 and 0.0073 less than the mean drift algorithm as a comparison, which significantly outperforms the mean drift algorithm in terms of the accuracy of the position and speed of the motion target tracking.

After completing the reliability verification of the Kalman joint filter fusion algorithm, the safety monitoring system of electrochemical energy storage power station applying the algorithm is further practiced to test the practical utility of the system. In the DST condition verification, the error of the estimated value of SOC is only about 4% compared with the real value, and the error of the variation curve of Li-ion battery internal resistance R_0 and the actual value of internal resistance is about 3%.In the UDDS condition verification, the error of the estimated value of SOC is only about 3% compared with the real value, and the error of the variation curve of Li-ion battery internal resistance R_0 and the actual value of internal resistance is about 3%. Obviously, the safety monitoring system of electrochemical energy storage power station constructed in this paper performs well in the intelligent operation and maintenance of energy storage power station, and the practical utility is excellent.

References

[1] Abomazid, A. M., El-Taweel, N. A., & Farag, H. E. (2022). Optimal energy management of hydrogen energy facility using integrated battery energy storage and solar photovoltaic systems. IEEE Transactions on Sustainable Energy, 13(3), 1457-1468.

[2] Gür, T. M. (2018). Review of electrical energy storage technologies, materials and systems: challenges and prospects for large-scale grid storage. Energy & Environmental Science, 11(10), 2696-2767.

[3] Chen, M., Zhang, Y., Xing, G., Chou, S. L., & Tang, Y. (2021). Electrochemical energy storage devices working in extreme conditions. Energy & Environmental Science, 14(6), 3323-3351.

[4] Elalfy, D. A., Gouda, E., Kotb, M. F., Bureš, V., & Sedhom, B. E. (2024). Comprehensive review of energy storage systems technologies, objectives, challenges, and future trends. Energy Strategy Reviews, 54, 101482.

[5] Zhang, C., Zhang, L., & Yu, G. (2020). Eutectic electrolytes as a promising platform for next-generation electrochemical energy storage. Accounts of Chemical Research, 53(8), 1648-1659.

[6] Jafarizadeh, H., Yamini, E., Zolfaghari, S. M., Esmaeilion, F., Assad, M. E. H., & Soltani, M. (2024). Navigating challenges in large-scale renewable energy storage: Barriers, solutions, and innovations. Energy Reports, 12, 2179-2192.

[7] Liu, J., Chen, X., Cao, S., & Yang, H. (2019). Overview on hybrid solar photovoltaic-electrical energy storage technologies for power supply to buildings. Energy conversion and management, 187, 103-121.

[8] Xiankui, W. E. N., Zhagn, S., Tongtian, D. E. N. G., Pan, L. I., & Wen, C. H. E. N. (2018). A summary of large capacity power energy storage peak regulation and frequency adjustment performance. Power Generation Technology, 39(6), 487.

[9] Lobato-Peralta, D. R., Okoye, P. U., & Alegre, C. (2024). A review on carbon materials for electrochemical energy storage applications: State of the art, implementation, and synergy with metallic compounds for

supercapacitor and battery electrodes. Journal of Power Sources, 617, 235140.

[10] Tan, K. M., Babu, T. S., Ramachandaramurthy, V. K., Kasinathan, P., Solanki, S. G., & Raveendran, S. K. (2021). Empowering smart grid: A comprehensive review of energy storage technology and application with renewable energy integration. Journal of Energy Storage, 39, 102591.

[11] Poizot, P., Gaubicher, J., Renault, S., Dubois, L., Liang, Y., & Yao, Y. (2020). Opportunities and challenges for organic electrodes in electrochemical energy storage. Chemical reviews, 120(14), 6490-6557.

[12] Rohit, A. K., Devi, K. P., & Rangnekar, S. (2017). An overview of energy storage and its importance in Indian renewable energy sector: Part I–Technologies and Comparison. Journal of Energy Storage, 13, 10-23.

[13] Ding, W., Bonk, A., & Bauer, T. (2018). Corrosion behavior of metallic alloys in molten chloride salts for thermal energy storage in concentrated solar power plants: A review. Frontiers of Chemical Science and Engineering, 12, 564-576.

[14] Zhang, Z., Ding, T., Zhou, Q., Sun, Y., Qu, M., Zeng, Z., ... & Chi, F. (2021). A review of technologies and applications on versatile energy storage systems. Renewable and Sustainable Energy Reviews, 148, 111263.

[15] Dong, W., & Huang, F. (2024). Understanding the influence of crystal packing density on electrochemical energy storage materials. eScience, 4(1), 100158.

[16] Jafari, M., Botterud, A., & Sakti, A. (2022). Decarbonizing power systems: A critical review of the role of energy storage. Renewable and Sustainable Energy Reviews, 158, 112077.

[17] Zu, L., Zhang, W., Qu, L., Liu, L., Li, W., Yu, A., & Zhao, D. (2020). Mesoporous materials for electrochemical energy storage and conversion. Advanced Energy Materials, 10(38), 2002152.

[18] Guney, M. S., & Tepe, Y. (2017). Classification and assessment of energy storage systems. Renewable and sustainable energy reviews, 75, 1187-1197.

[19] Lv, Z., Li, W., Yang, L., Loh, X. J., & Chen, X. (2019). Custom-made electrochemical energy storage devices. ACS Energy Letters, 4(2), 606-614.

[20] Smith, K., Saxon, A., Keyser, M., Lundstrom, B., Cao, Z., & Roc, A. (2017, May). Life prediction model for grid-connected Li-ion battery energy storage system. In 2017 American Control Conference (ACC) (pp. 4062-4068). IEEE.

[21] Wang, F., Ouyang, D., Zhou, Z., Page, S. J., Liu, D., & Zhao, X. (2021). Lignocellulosic biomass as sustainable feedstock and materials for power generation and energy storage. Journal of Energy Chemistry, 57, 247-280.

[22] Koohi-Fayegh, S., & Rosen, M. A. (2020). A review of energy storage types, applications and recent developments. Journal of Energy Storage, 27, 101047.

[23] Wang, B., Ruan, T., Chen, Y., Jin, F., Peng, L., Zhou, Y., ... & Dou, S. (2020). Graphene-based composites for electrochemical energy storage. Energy storage materials, 24, 22-51.

[24] Bullich-Massagué, E., Cifuentes-García, F. J., Glenny-Crende, I., Cheah-Mañé, M., Aragüés-Peñalba, M., Díaz-González, F., & Gomis-Bellmunt, O. (2020). A review of energy storage technologies for large scale photovoltaic power plants. Applied Energy, 274, 115213.

[25] Amirante, R., Cassone, E., Distaso, E., & Tamburrano, P. (2017). Overview on recent developments in energy storage: Mechanical, electrochemical and hydrogen technologies. Energy Conversion and Management, 132, 372-387.

[26] Shi, X., Das, P., & Wu, Z. S. (2021). Digital microscale electrochemical energy storage devices for a fully connected and intelligent world. ACS Energy Letters, 7(1), 267-281.

[27] Byrne, R. H., Nguyen, T. A., Copp, D. A., Chalamala, B. R., & Gyuk, I. (2017). Energy management and optimization methods for grid energy storage systems. IEEE Access, 6, 13231-13260.

[28] Zame, K. K., Brehm, C. A., Nitica, A. T., Richard, C. L., & Schweitzer III, G. D. (2018). Smart grid and energy storage: Policy recommendations. Renewable and sustainable energy reviews, 82, 1646-1654.

[29] Kaabeche, A., & Bakelli, Y. (2019). Renewable hybrid system size optimization considering various electrochemical energy storage technologies. Energy conversion and management, 193, 162-175.

[30] Zhang, C., Wei, Y. L., Cao, P. F., & Lin, M. C. (2018). Energy storage system: Current studies on batteries and power condition system. Renewable and Sustainable Energy Reviews, 82, 3091-3106.

[31] Rashidi, S., Karimi, N., Sunden, B., Kim, K. C., Olabi, A. G., & Mahian, O. (2022). Progress and challenges on the thermal management of electrochemical energy conversion and storage technologies: Fuel cells, electrolysers, and supercapacitors. Progress in Energy and Combustion Science, 88, 100966.

[32] Abdalla, A. N., Nazir, M. S., Tao, H., Cao, S., Ji, R., Jiang, M., & Yao, L. (2021). Integration of energy storage system and renewable energy sources based on artificial intelligence: An overview. Journal of Energy Storage, 40, 102811.

[33] CHENG, Z., CAO, W., HU, B., CHENG, Y., LI, X., JIANG, L., ... & WANG, Q. (2023). Thermal runaway and explosion propagation characteristics of large lithium iron phosphate battery for energy storage station. Energy Storage Science and Technology, 12(3), 923.

[34] Barry W. Mulvey & Thrishantha Nanayakkara. (2024). HAVEN: Haptic And Visual Environment Navigation by a Shape-Changing Mobile Robot with Multimodal Perception. Scientific Reports(1),27018-27018.

[35] Jinyue Liu,Xiong Tan,Xiaohui Jia,Tiejun Li & Wei Li. (2024). A gait phase recognition method for obstacle crossing based on multi-sensor fusion. Sensors and Actuators: A. Physical115645-115645.

[36] Anuj Kumar & Velagapudi Vasu. (2024). Tool wear prediction using multi-sensor data fusion and attention-based deep learning. Production Engineering(prepublish),1-17.

[37] ReshmaKunjumon & SangeethaGopan G. S. (2021). Implementation of Vision and Lidar Sensor Fusion Using Kalman Filter Algorithm. International Journal of Sciences: Basic and Applied Research (IJSBAR)(2),183-198.

[38] El Aabaribaoune Mohammad,Emili Emanuele & Guidard Vincent. (2021). Estimation of the error covariance matrix for IASI radiances and its impact on the assimilation of ozone in a chemistry transport model. Atmospheric Measurement Techniques(4),2841-28.